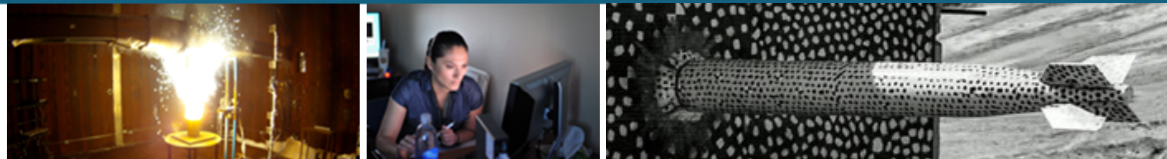




Artificial Intelligence and Machine Learning Support for Probabilistic Fracture Mechanics Analysis



Stephen J. Verzi, Joseph P. Lubars,
Satyanadh Gundimada, Michael J. Starr

Sandia National Laboratories

Matthew Homiack, Raj Iyengar

U.S. Nuclear Regulatory Commission

Machine Learning / Deep Learning Workshop July 17-20, 2023



This presentation was prepared as an account of work sponsored by an agency of the U.S. Government. Neither the U.S. Government nor any agency thereof, nor any of their employees, makes any warranty, expressed or implied, or assumes any legal liability or responsibility for any third party's use, or the results of such use, of any information, apparatus, product, or process disclosed in this report, or represents that its use by such third party would not infringe privately owned rights. The views expressed in this presentation are not necessarily those of the U.S. Nuclear Regulatory Commission.

U.S. DEPARTMENT OF ENERGY
NNSA
Sandia National Laboratories is a multimission laboratory managed and operated by National Technology and Engineering Solutions of Sandia, a wholly owned subsidiary of Honeywell International Inc. for the U.S. Department of Energy's National Nuclear Security Administration under contract DE-NA0003525.

Abstract



In this research, artificial intelligence and machine learning (ML) methods are used to search an uncertain parameter space more efficiently for the most important inputs with respect to response sensitivities and then to construct, train, and test low-fidelity surrogate models. These methods are applied to the Extremely Low Probability of Rupture (xLPR) probabilistic fracture mechanics code used at the U.S. Nuclear Regulatory Commission in support of nuclear regulatory research. This presentation will show two separate but related efforts: 1) ranking important uncertain input features with respect to target outputs as determined by convergence in the confidence intervals for increasing sample sizes using simple random sampling; and 2) implementation of a reduced-order surrogate model for fast, approximate sample generation. Unoptimized, readily available off-the-shelf ML models were used in both efforts.

The results show that ML models can assist analysts in conducting sensitivity and uncertainty analyses with respect to typical xLPR use cases. The ML models help to reduce the number of random realizations needed in the xLPR simulation by focusing on the most important input parameters (as part of the first effort) and augment xLPR output generation by providing quick approximate time-series simulation (as part of the second effort). This research involved several different kinds of ML models, including linear, random forest, gradient boosting, and multi-layer perceptron regression techniques. Even though not all models perform well in each task or scenario, especially when data is scarce (i.e., low probabilities of leak and rupture), the results show that there are cases where each ML model can perform well. Future efforts can focus on hyperparameter optimization, when appropriate. Both efforts were intended to augment xLPR simulations, which is what the results show.



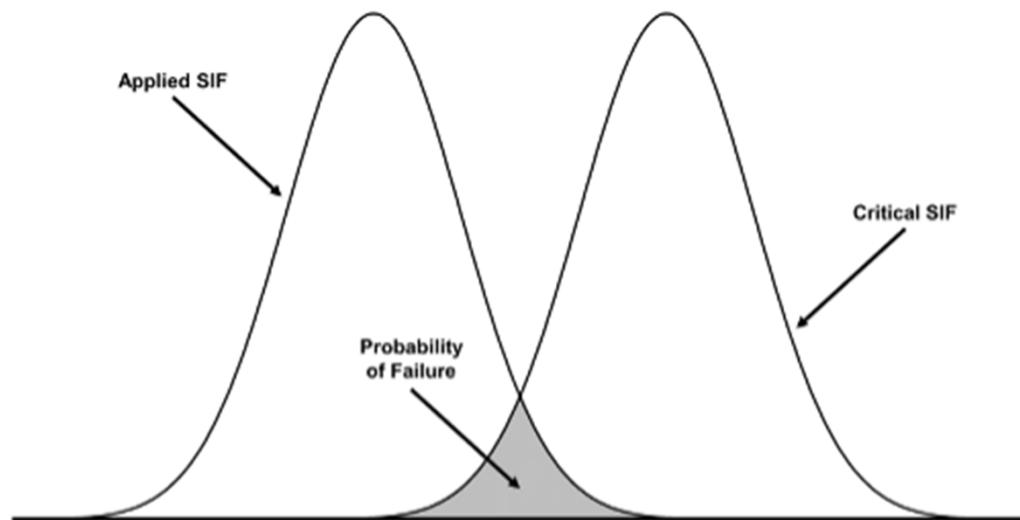
Outline

- Problem Space
 - Probabilistic Fracture Mechanics (PFM)
 - Extremely Low Probability of Rupture (xLPR) Code
- Solution Space
 - Artificial Intelligence (AI) and Machine Learning (ML)
 - Sensitivity Analysis with xLPR
 - Importance Sampling
 - Determining Appropriate Sample Size
 - Surrogate Model for xLPR Quantities of Interest (QoIs)
 - Time of 1st Leak, if any
 - Crack Propagation via Normalized Depth
- Results
- Potential Future Work
- Acknowledgments and Contacts



Problem Space – Probabilistic Fracture Mechanics (PFM)

- Analysis



This figure illustrates a simplistic PFM analysis. The curve on the left represents the distribution of crack driving force or applied stress intensity factor (SIF), which depends on the uncertainties in stress and crack size. The curve on the right represents the toughness distribution or critical (i.e., allowable) SIF of the material. When the two distributions overlap, there is a finite probability of failure, which is indicated by the shaded area. Time dependent crack growth, such as from fatigue or stress-corrosion cracking or both, can be considered by applying the appropriate growth laws to the crack distribution. Crack growth can cause the applied SIF distribution to shift to the right with time, thereby increasing the probability of failure.

Figure from U.S. NRC Technical Letter Report, TRL-RES/DE/REB-2022-13.



Problem Space – Extremely Low Probability of Rupture (xLPR) Code

- Analysis Architecture

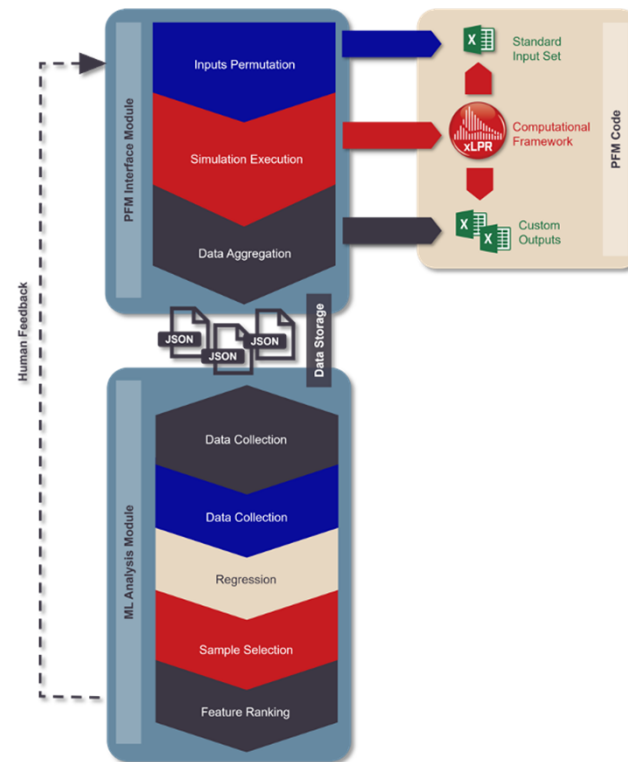


Figure from U.S. NRC Technical Letter Report, TRL-RES/DE/REB-2022-13.



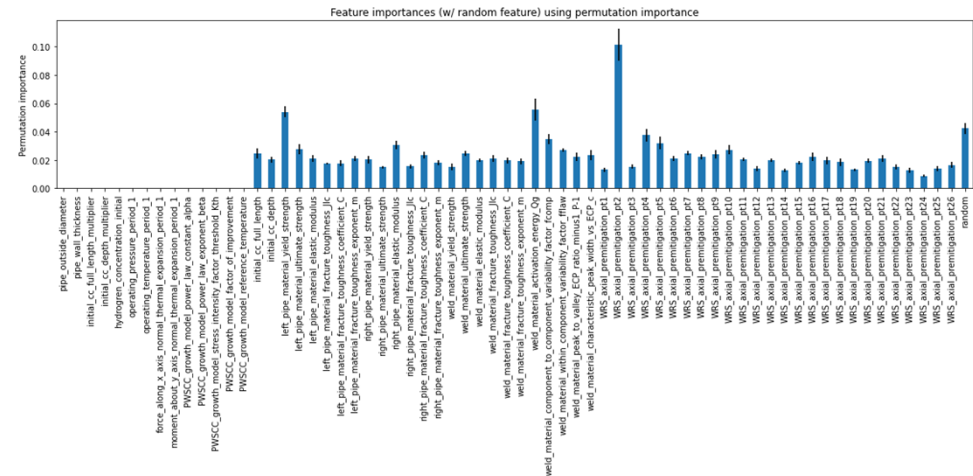
Sensitivity Analysis with xLPR

- Given input (uncertain parameter) distributions and associated Monte Carlo outputs
- Can we use AI/ML models to determine/rank importance of inputs while finding proper sample size with respect to output set?

Case	Input	Output	Method	Description
Bc 1 Welding Leak Rate DMS	1.16	3.21	Chromsteel and A54	Assess the base likelihood of failure caused by PWSCC initiation and growth without mechanical mitigation.
	1.16	3.22	Chromsteel and A54	Initial Flow Stress (1 A54 and 1 C10, Case)
	3.10	3.31	Chromsteel and A54	Assess the base likelihood of failure caused by PWSCC initiation and growth without mechanical mitigation.
Bc 2 Welding Leak Rate DMS	3.12	3.33	Chromsteel and A54	Assess the base likelihood of failure caused by PWSCC initiation and growth without mechanical mitigation.
	3.13	3.34	Chromsteel and A54	Assess the base likelihood of failure caused by PWSCC initiation and growth without mechanical mitigation.
	3.14	3.35	Chromsteel and A54	Assess the base likelihood of failure caused by PWSCC initiation and growth without mechanical mitigation.
Bc 3 Welding Leak Rate DMS	3.15	3.36	Chromsteel and A54	Assess the base likelihood of failure caused by PWSCC initiation and growth without mechanical mitigation.
	3.16	3.37	Chromsteel and A54	Assess the base likelihood of failure caused by PWSCC initiation and growth without mechanical mitigation.
	3.17	3.38	Chromsteel and A54	Assess the base likelihood of failure caused by PWSCC initiation and growth without mechanical mitigation.

Case	Input	Output	Method	Description
Bc 4 Welding Leak Rate DMS	5.10	3.61	Chromsteel and A54	Assess the base likelihood of failure caused by PWSCC initiation and growth without mechanical mitigation.
	5.11	3.62	Chromsteel and A54	Initial Flow Stress (1 A54 and 1 C10, Case)
	5.12	3.63	Chromsteel and A54	Assess the base likelihood of failure caused by PWSCC initiation and growth without mechanical mitigation.
Bc 5 Welding Leak Rate DMS	5.20	3.71	Chromsteel and A54	Assess the base likelihood of failure caused by PWSCC initiation and growth without mechanical mitigation.
	5.21	3.72	Chromsteel and A54	Initial Flow Stress (1 A54 and 1 C10, Case)
	5.22	3.73	Chromsteel and A54	Assess the base likelihood of failure caused by PWSCC initiation and growth without mechanical mitigation.

inputs



NRC, Technical Letter Report TLR-RES/DE/REB-2021-14-R1, "Probabilistic Leak-Before-Break Evaluations of Pressurized-Water Reactor Piping Systems using the Extremely Low Probability of Rupture Code," April 2022, ADAMS Accession No. ML22088A006



Surrogate Modeling using ML for xLPR

- Given input (uncertain parameter) distributions and associated Monte Carlo outputs
 - Can we use AI/ML models to train surrogate model with respect to output set?

Outputs or Quantities of Interest (QoIs)

cc_depth_normalized

cc_ID_length_normalized

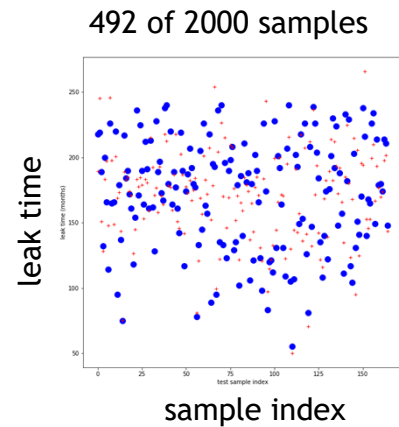
cc_OD_length_normalized

is_leaking

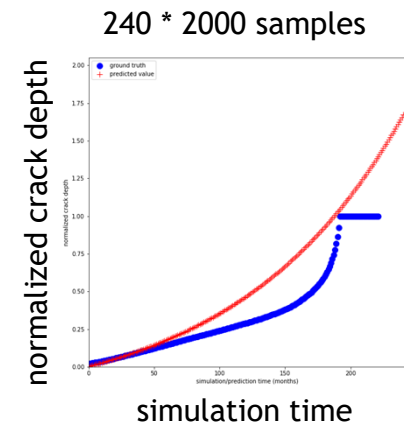
is_ruptured

total_leak_rate

outputs



potential surrogate models



Results

- Using random forest regressor (scikit-learn)
 - Mean decrease in impurity (MDI)
 - Permutation importance values
- Using linear regression (scikit-learn)

Outputs or Quantities of Interest (QoIs)

cc_depth_normalized

cc_ID_length_normalized

cc_OD_length_normalized

is_leaking

is_ruptured

total_leak_rate

```

pipe_outside_diameter
pipe_wall_thickness
initial_cc_full_length_multiplier
initial_cc_depth_multiplier
hydrogen_concentration_initial
operating_pressure_period_1
operating_temperature_period_1
force_along_x_axis_normal_thermal_expansion_period_1
moment_about_y_axis_normal_thermal_expansion_period_1
PWSCC_growth_model_power_law_constant_alpha
PWSCC_growth_model_power_law_exponent_beta
PWSCC_growth_model_stress_intensity_factor_threshold_Kth
PWSCC_growth_model_factor_of_improvement
PWSCC_growth_model_reference_temperature
initial_cc_full_length
initial_cc_depth
left_pipe_material_yield_strength
left_pipe_material_ultimate_strength
left_pipe_material_elastic_modulus
left_pipe_material_fracture_toughness_JIc
left_pipe_material_fracture_toughness_coefficient_C
left_pipe_material_fracture_toughness_exponent_m
right_pipe_material_yield_strength
right_pipe_material_ultimate_strength
right_pipe_material_elastic_modulus
right_pipe_material_fracture_toughness_JIc
right_pipe_material_fracture_toughness_coefficient_C
right_pipe_material_fracture_toughness_exponent_m
weld_material_yield_strength
weld_material_ultimate_strength
weld_material_elastic_modulus
weld_material_fracture_toughness_JIc
weld_material_fracture_toughness_coefficient_C
weld_material_fracture_toughness_exponent_m
weld_material_activation_energy_Dg
weld_material_component_to_component_variability_factor_fcomp
weld_material_within_component_variability_factor_fflaw
weld_material_peak_to_valley_ECP_ratio_minus_1_P-1
weld_material_characteristic_peak_width_vs_ECP_c
WRS_axial_premitigation_pt1
WRS_axial_premitigation_pt2
WRS_axial_premitigation_pt3
WRS_axial_premitigation_pt4
WRS_axial_premitigation_pt5
WRS_axial_premitigation_pt6
WRS_axial_premitigation_pt7
WRS_axial_premitigation_pt8
WRS_axial_premitigation_pt9
WRS_axial_premitigation_pt10
WRS_axial_premitigation_pt11
WRS_axial_premitigation_pt12
WRS_axial_premitigation_pt13
WRS_axial_premitigation_pt14
WRS_axial_premitigation_pt15
WRS_axial_premitigation_pt16
WRS_axial_premitigation_pt17
WRS_axial_premitigation_pt18
WRS_axial_premitigation_pt19
WRS_axial_premitigation_pt20
WRS_axial_premitigation_pt21
WRS_axial_premitigation_pt22
WRS_axial_premitigation_pt23
WRS_axial_premitigation_pt24
WRS_axial_premitigation_pt25
WRS_axial_premitigation_pt26

```

inputs



9 Results – Using Random Forest Regressor

- Multi-variate output set (6) given input set (65) w/ 200 samples

Input Variable	Permutation Importance
WRS_axial_premitigation_pt01	0.5973
WRS_axial_premitigation_pt26	0.0680
WRS_axial_premitigation_pt24	0.0545
WRS_axial_premitigation_pt22	0.0501
WRS_axial_premitigation_pt05	0.0351
weld_material_PWSCC_growth_component_to_component_variability_factor_fcomp	0.0280
WRS_axial_premitigation_pt21	0.0255
weld_material_PWSCC_growth_activation_energy_Qg	0.0202
WRS_axial_premitigation_pt02	0.0158
WRS_axial_premitigation_pt07	0.0133
WRS_axial_premitigation_pt17	0.0107

Ranked permutation importance for those inputs with values greater than random feature mean + 2 * standard deviation.



Results – Using Random Forest Regressor

- Multi-variate output set (6) given input set (65) w/ 2000 samples

Input Variable	Permutation Importance
WRS_axial_premitigation_pt01	0.9740
weld_material_PWSCC_growth_component_to_component_variability_factor_fcomp	0.2029
weld_material_PWSCC_growth_within_component_variability_factor_fflaw	0.1503
WRS_axial_premitigation_pt14	0.0301
WRS_axial_premitigation_pt26	0.0268
WRS_axial_premitigation_pt22	0.0230
WRS_axial_premitigation_pt02	0.0176
WRS_axial_premitigation_pt23	0.0163
WRS_axial_premitigation_pt24	0.0162
WRS_axial_premitigation_pt07	0.0158

Ranked permutation importance for those inputs with values greater than random feature mean + 2 * standard deviation.



Results – Using Random Forest Regressor

- Multi-variate output set (6) given input set (65) w/ 20000 samples

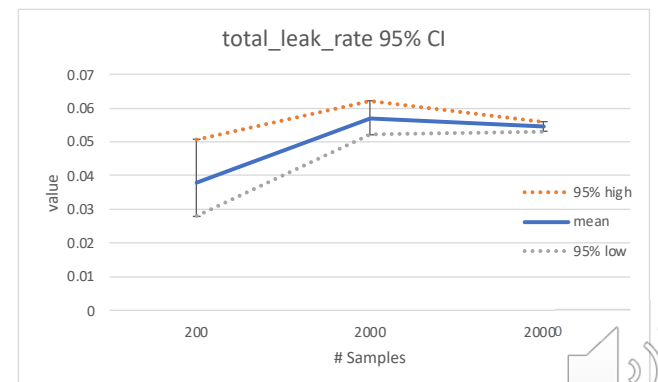
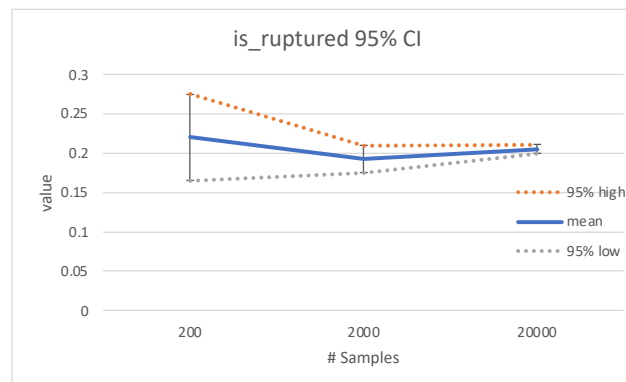
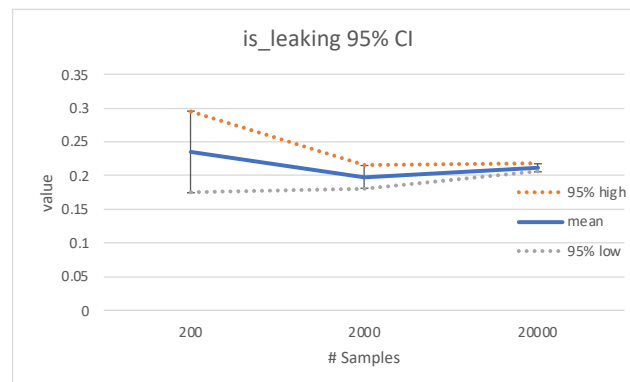
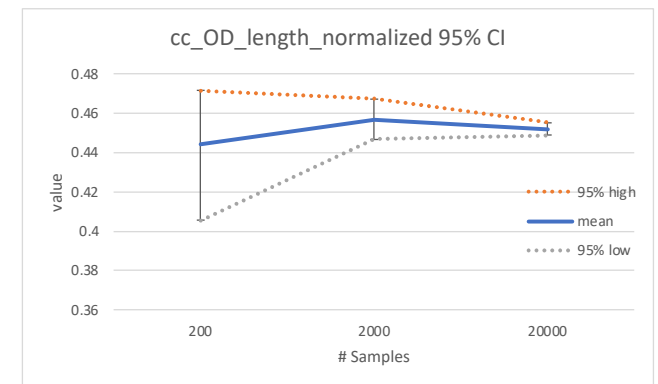
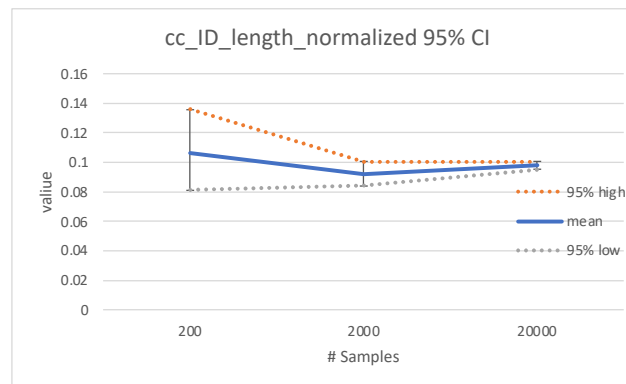
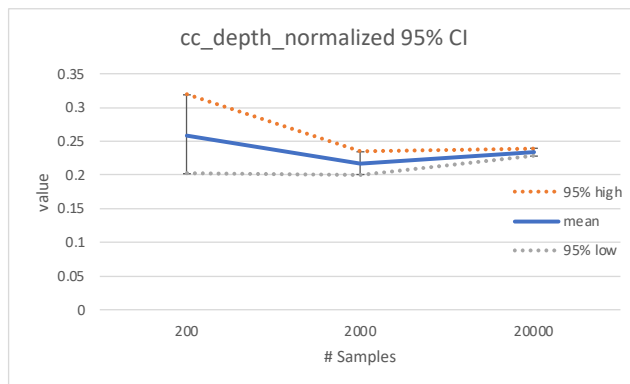
Input Variable	Permutation Importance
WRS_axial_premitigation_pt01	1.2146
weld_material_PWSCC_growth_component_to_component_variability_factor_fcomp	0.3489
weld_material_PWSCC_growth_within_component_variability_factor_fflaw	0.2416
WRS_axial_premitigation_pt02	0.1115
initial_cc_full_length	0.0323
WRS_axial_premitigation_pt25	0.0226
weld_material_PWSCC_growth_activation_energy_Qg	0.0205
WRS_axial_premitigation_pt26	0.0177
WRS_axial_premitigation_pt24	0.0162
left_pipe_material_yield_strength	0.0155

Ranked permutation importance for those inputs with values greater than random feature mean + 2 * standard deviation.



Results – Using Random Forest Regressor

- Determining appropriate sample size (all 6 QoIs) – Confidence intervals for 200, 2000 and 20000 samples



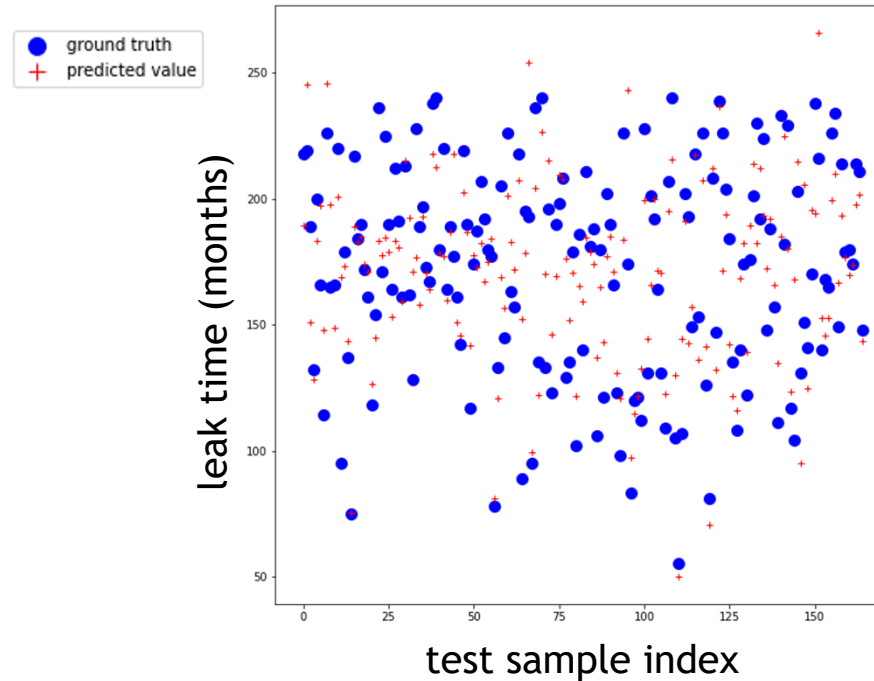
2000 Samples are sufficient



Results – Using Linear Regression

- 492 (out of 2000) samples – 75/25 % training/testing split

Predicted leak time (in months) for test set by sample index



Seems like we do not have enough training data

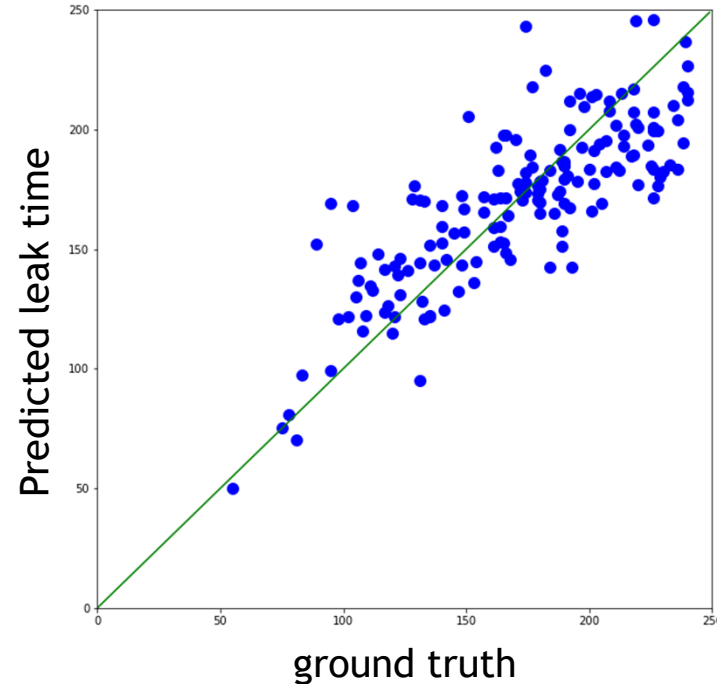
mse = 662.7



Results – Using Linear Regression

- 492 (out of 2000) samples – 75/25 % training/testing split

Ground truth versus predicted for test set by sample



Seems like we do not have enough training data

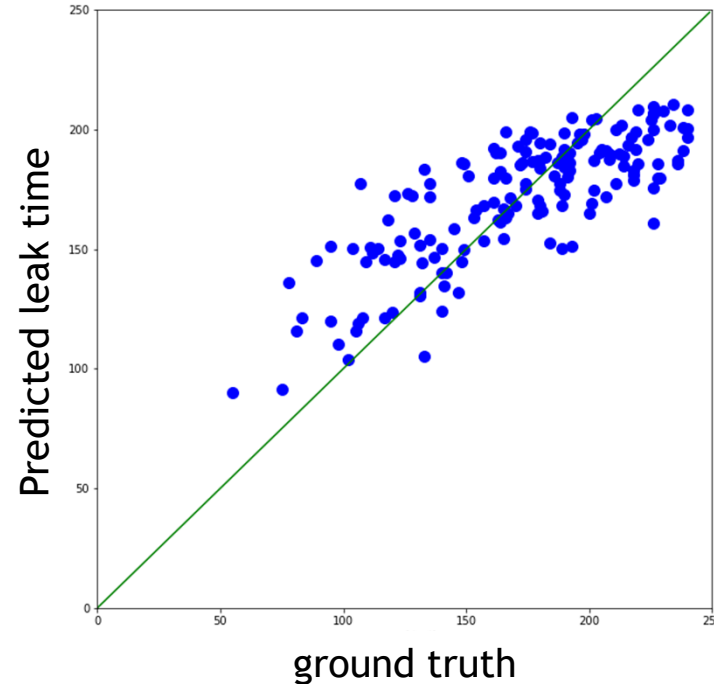
mse = 662.7



Results – Using Random Forest Regression

- 492 (out of 2000) samples – 75/25 % training/testing split

Ground truth versus predicted for test set by sample



Seems to miss both high and low values (we probably do not have enough training data)

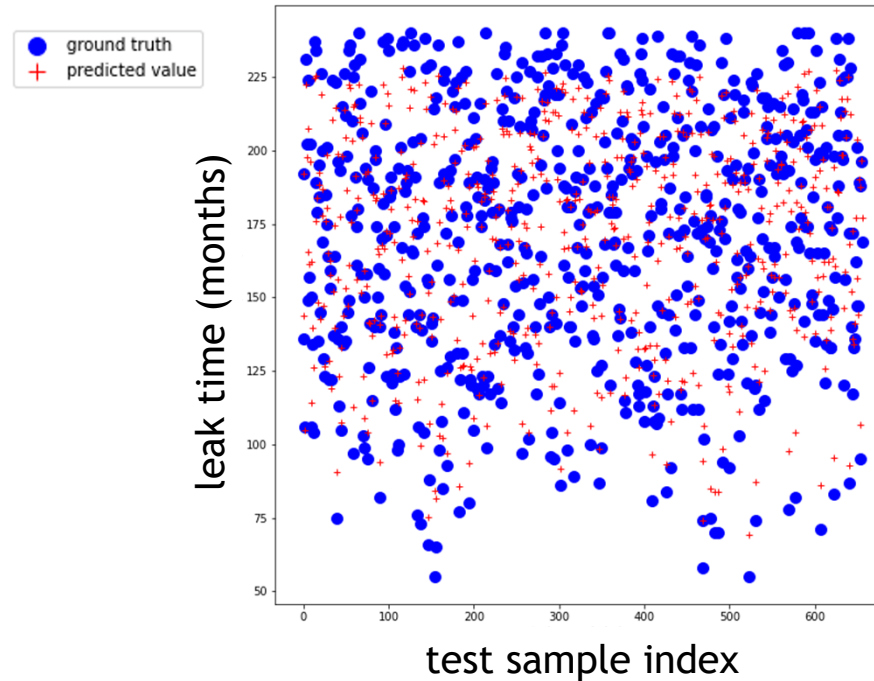
mse = 707.5



Results – Using Random Forest Regression

- 492 (out of 2000) samples – 100/0 % training/testing split

Predicted leak time (in months) for train set by sample index



Significant drop
in mse

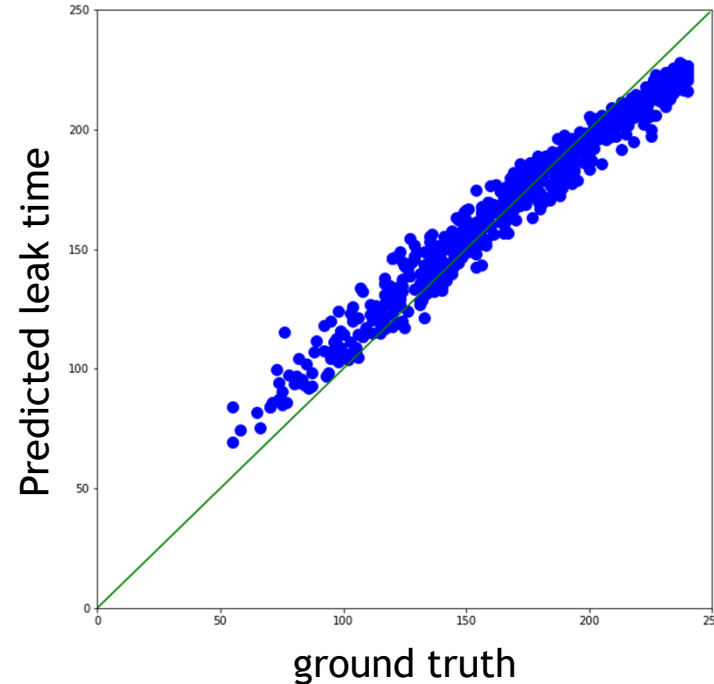
mse = 108.6



Results – Using Random Forest Regression

- 492 (out of 2000) samples – 100/0 % training/testing split

Ground truth versus predicted for train set by sample



Significant drop
in mse - but
model still not
capturing high
and low ends
well

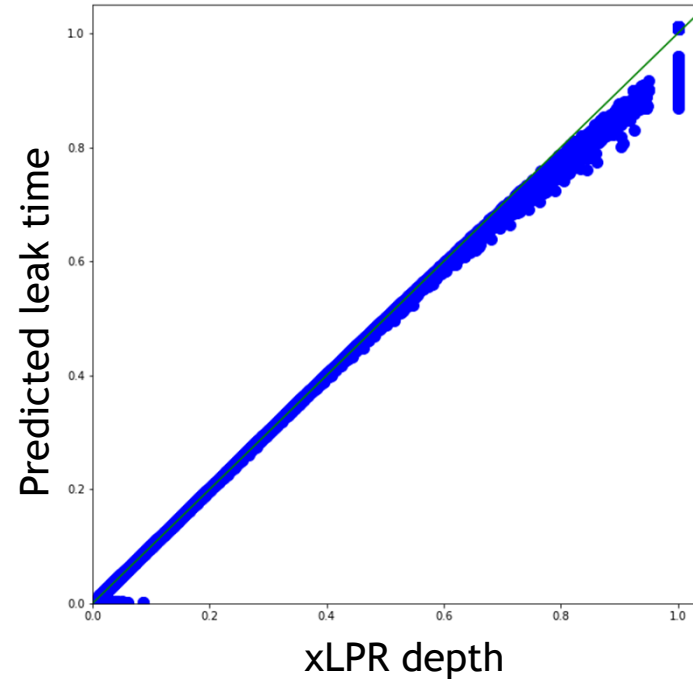
mse = 108.6



Results – Using Linear Regression

- 2000 samples – 75/25 % training/testing split

xLPR depth versus predicted for test set by sample



Seems to lose performance for larger normalized crack depth values

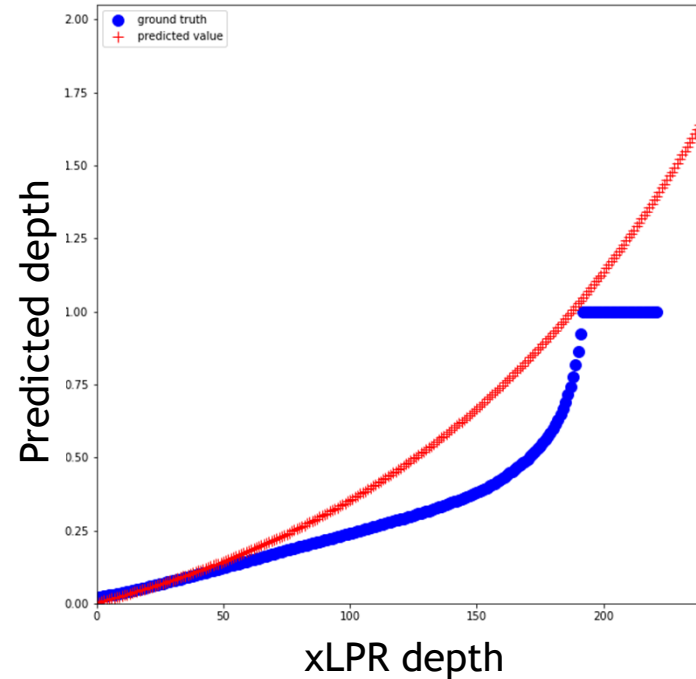
mse = $2.7e-5$



Results – Using Linear Regression

- 2000 samples – 75/25 % training/testing split

xLPR depth versus predicted time-series for single sample initial conditions



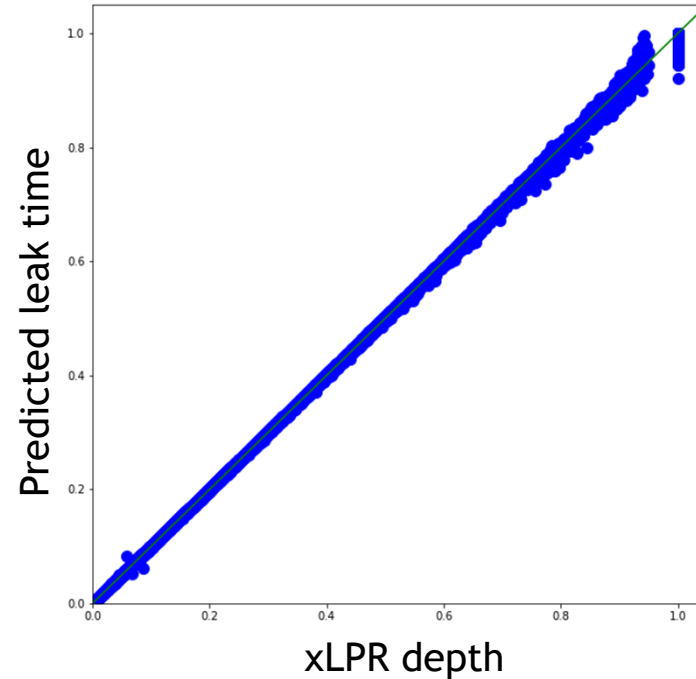
Attempts to extrapolate beyond unit normalized crack depth



Results – Using Random Forest Regression

- 2000 samples – 75/25 % training/testing split

xLPR depth versus predicted for test set by sample



Captures larger normalized crack depth values and more of curvature

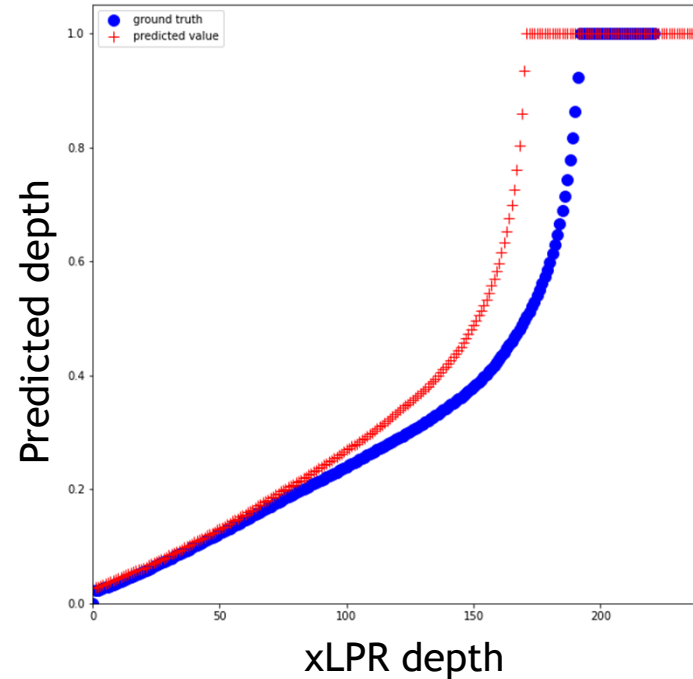
mse = 2.0e-6



Results – Using Random Forest Regression

- 2000 samples – 75/25 % training/testing split

xLPR depth versus predicted time-series for single sample initial conditions



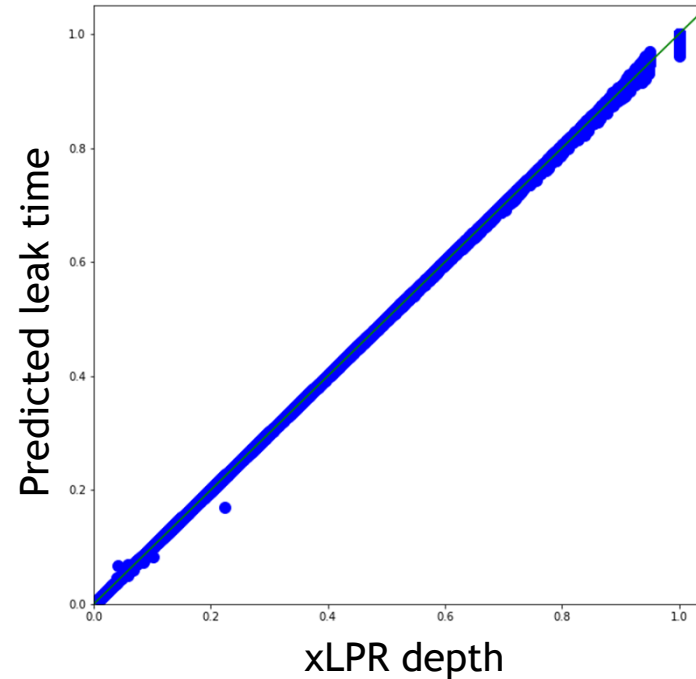
Captures similar curvature, but predicts leak sooner than xLPR



Results – Using Random Forest Regression

- 2000 samples – train and test on 100% of data

xLPR depth versus predicted for train set by sample



Captures larger normalized crack depth, but with increased uncertainty

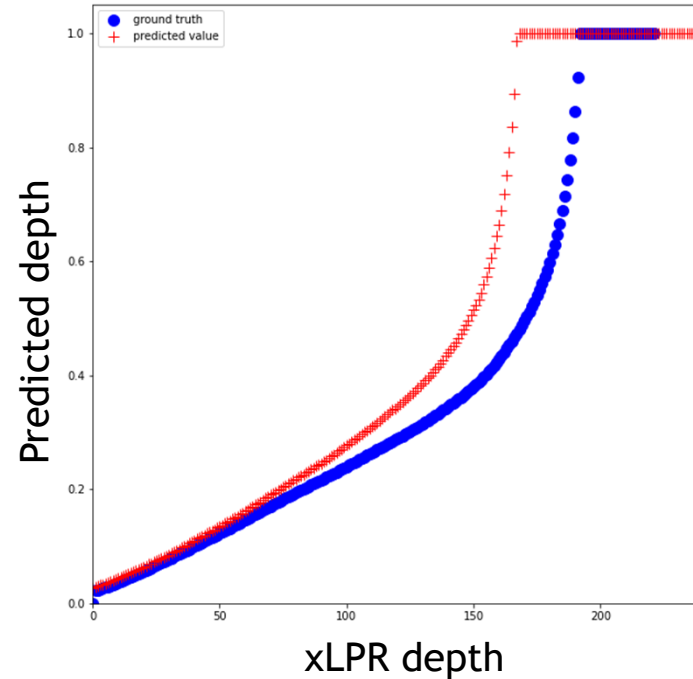
mse = $2.5e-7$



Results – Using Random Forest Regression

- 2000 samples – train and test on 100% of data

xLPR depth versus predicted time-series for single sample initial conditions



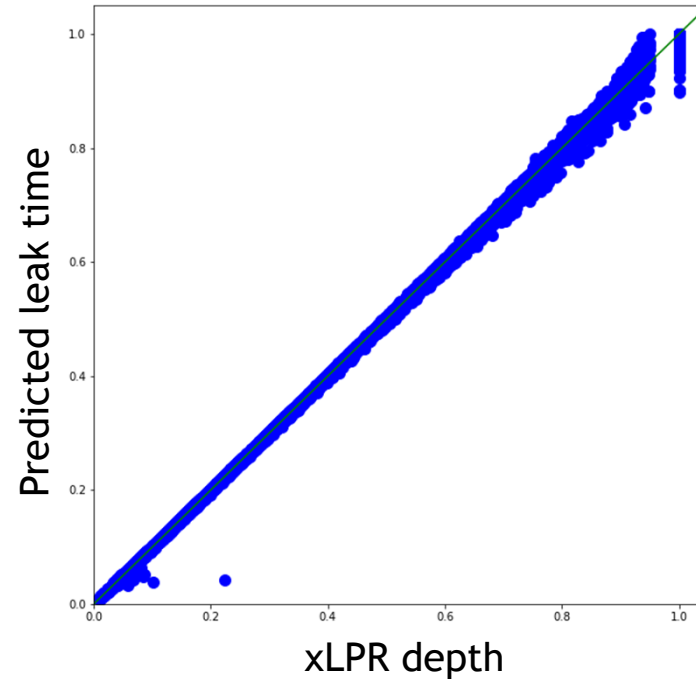
Captures similar curvature, but predicts leak “even” sooner than xLPR or 75% training data - indicates overtraining



Results – Using Random Forest Regression

- 2000 samples – 25/75 % training/testing split

xLPR depth versus predicted for test set by sample



Captures larger normalized crack depth values but with increased uncertainty

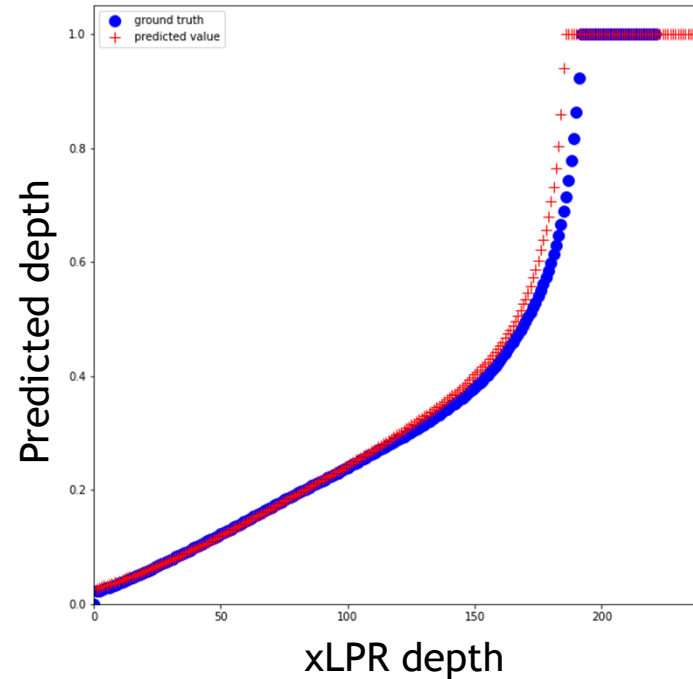
mse = $2.7e-6$



Results – Using Random Forest Regression

- 2000 samples – 25/75 % training/testing split

xLPR depth versus predicted time-series for single sample initial conditions



Captures similar curvature, but predicts leak sooner than xLPR - not as overtrained



Potential Future Work

- Efficiently identify response sensitivities from an uncertain input parameter space
 - Sensitivity analysis
 - Sensitivity studies
 - Uncertainty analysis
- Identify methods of creating tiered surrogate models (machine-learning/data-driven) with comparable accuracy to the physics-based xLPR model, including characterization of the increased computational efficiency of the potential surrogate models
 - Start with one output and use neural network to predict
 - Determine level of effort needed



Our Team – Sandia



Sandia

- Michael Starr (PI)
- Stephen Verzi (staff, ML)
- Joseph Lubars (staff, ML/RL & statistics)
- Satyanadh Gundimada (staff, ML/DL)

U.S. Nuclear Regulatory Commission

- Matthew Homiack
- Raj Iyengar

Sandia National Laboratories is a multimission laboratory managed and operated by National Technology and Engineering Solutions of Sandia LLC, a wholly owned subsidiary of Honeywell International Inc. for the U.S. Department of Energy's National Nuclear Security Administration under contract DE-NA0003525.

This presentation was prepared as an account of work sponsored by an agency of the U.S. Government. Neither the U.S. Government nor any agency thereof, nor any of their employees, makes any warranty, expressed or implied, or assumes any legal liability or responsibility for any third party's use, or the results of such use, of any information, apparatus, product, or process disclosed in this report, or represents that its use by such third party would not infringe privately owned rights. The views expressed in this presentation are not necessarily those of the U.S. Nuclear Regulatory Commission.



Thank You

- Questions?

